

Investigating the Effect of Neutrino Decay on Flavor Oscillations

Chloe Klare¹  and André de Gouvêa²

Published 2020 September 15 • © 2020. The American Astronomical Society. All rights reserved.

Research Notes of the AAS, Volume 4, Number 9

Citation Chloe Klare and André de Gouvêa 2020 *Res. Notes AAS* **4** 154

¹ Department of Aerospace, Physics, and Space Sciences, Florida Institute of Technology, 150 W University Boulevard, Melbourne, FL 32901, USA

² Department of Physics and Astronomy, Northwestern University, 2145 Sheridan Road, Evanston, IL 60208, USA

Chloe Klare  <https://orcid.org/0000-0002-8899-3769>

Received 2020 September 9

Accepted 2020 September 12

Published 2020 September 15

<https://doi.org/10.3847/2515-5172/abb812>

Neutrino oscillations ; Neutrino masses

 Journal RSS

[Sign up for new issue notifications](#)

[Create citation alert](#)

Export citation and abstract

[BibTeX](#)

[RIS](#)

1. Introduction

As our knowledge of neutrinos has grown significantly in recent decades, so has the number of open questions in neutrino physics. For example, we know that neutrinos are massive particles which oscillate between different flavor states, but we are still learning how this happens in detail (de Gouvêa 2008). There are three types of neutrinos, called flavor states, which any given neutrino oscillates between: electron-type, muon-type, and tau-type (de Gouvêa 2008). Each flavor state is represented by a linear combination of mass states, denoted $|\nu_1\rangle$, $|\nu_2\rangle$, and $|\nu_3\rangle$ (de Gouvêa 2008). Only electron-type antineutrinos are visible to a reactor neutrino detector, so here we focus on the probability that a neutrino will remain an electron-type neutrino. This probability is given by Equation (1), where $|\nu(L)\rangle$ (Equation (2)) represents the state of the neutrino after traveling a distance L (de Gouvêa 2008).

$$P_{ee} = |\langle \nu_e | \nu(L) \rangle|^2 \quad (1)$$

$$\begin{aligned} |\nu(L)\rangle &= \cos \theta_{12} \cos \theta_{13} e^{-im_1^2 L/2E} |\nu_1\rangle \\ &+ \sin \theta_{12} \cos \theta_{13} e^{-im_2^2 L/2E} |\nu_2\rangle \\ &+ \sin \theta_{13} e^{-i\delta} e^{-im_3^2 L/2E} |\nu_3\rangle. \end{aligned} \quad (2)$$

Using this relationship, we calculated this probability to be, in natural units ($\hbar = c = 1$):

$$P_{ee} = 1 - \sin^2 2\theta_{12} \cos^4 \theta_{13} \sin^2 \left(\frac{\Delta m_{21}^2 L}{4E} \right) - \sin^2 2\theta_{13} \left(\sin^2 \theta_{12} \sin^2 \left(\frac{\Delta m_{32}^2 L}{4E} \right) + \cos^2 \theta_{12} \sin^2 \left(\frac{\Delta m_{31}^2 L}{4E} \right) \right) \quad (3)$$

where Δm_{ij}^2 is the mass-squared difference between ν_i and ν_j , θ_{12} and θ_{13} are lepton mixing angles, and E represents the detected antineutrino energy. This probability function is characterized by two distinct oscillations: long oscillations driven by Δm_{21}^2 and $\sin^2 \theta_{12}$ and short oscillations driven by Δm_{31}^2 and $\sin^2 \theta_{13}$. When L is expressed in meters, Δm^2 in eV^2/c^4 , and E in MeV, the arguments of the sine functions in Equation (3) are given by $1.267\Delta m^2 L/E$.

Here, we investigated the effects of neutrino mass eigenstate decay on the flavor oscillations, and we determined bounds on the neutrino lifetimes. We predict our lifetime estimates can be tested by the Jiangmen Underground Neutrino Observatory (JUNO) experiment. JUNO, which is under construction, will be the first neutrino observatory with both the large baseline necessary to detect the long oscillations and the high resolution required to observe the small oscillations (An et al. 2016). Our research consists of simulating data to be collected by the JUNO experiment.

2. Neutrino Decay

Unless otherwise noted, we chose the following values of our parameters, which we obtained from An et al. (2016) to more easily compare our results with those from the JUNO collaboration:

$$\begin{aligned} \theta_{12} &= 33.7^\circ \\ \theta_{13} &= 8.8^\circ \\ \Delta m_{21}^2 &= 7.54 \times 10^{-5} \text{ eV}^2 \\ \Delta m_{32}^2 &= 2.40 \times 10^{-3} \text{ eV}^2 \\ L &= 52,000 \text{ m.} \end{aligned}$$

Additionally, in our data analysis, we sorted our values into 50 energy bins, maintaining a bin width of 0.1 MeV, which agrees with JUNO's energy resolution (An et al. 2016).

We derived the probability function in the cases where each mass state decays, which we compared to the original model. We assumed the daughter particles of the decaying neutrinos are invisible to the detector. To model the decay, we introduced a decay factor of $m\Gamma$, which is related to the neutrino lifetime by $m\Gamma = m/\tau$, where τ is the lifetime. In the case where each neutrino has a finite lifetime, we let

$$\begin{aligned} |\nu(L)\rangle &= \cos \theta_{12} \cos \theta_{13} e^{-im_1^2 L/2E} e^{-\frac{m_1 \Gamma_1 L}{2E}} |\nu_1\rangle \\ &+ \sin \theta_{12} \cos \theta_{13} e^{-im_2^2 L/2E} e^{-\frac{m_2 \Gamma_2 L}{2E}} |\nu_2\rangle \\ &+ \sin \theta_{13} e^{-i\delta} e^{-im_3^2 L/2E} e^{-\frac{m_3 \Gamma_3 L}{2E}} |\nu_3\rangle. \end{aligned} \quad (4)$$

Using Equation (1), we calculated our probability function, including the effect of neutrino decay, to be:

$$\begin{aligned} P_{ee} &= c_{12}^4 c_{13}^4 \exp \left(-\frac{m_1 \Gamma_1 L}{E} \right) + s_{12}^4 c_{13}^4 \exp \left(-\frac{m_2 \Gamma_2 L}{E} \right) + s_{13}^4 \\ &\times \exp \left(-\frac{m_3 \Gamma_3 L}{E} \right) + 2c_{12}^2 s_{12}^2 c_{13}^4 \exp \left(-\frac{L(m_1 \Gamma_1 + m_2 \Gamma_2)}{2E} \right) \\ &\times \left(1 - 2 \sin^2 \frac{\Delta m_{21}^2 L}{4E} \right) + 2c_{12}^2 c_{13}^2 s_{13}^2 \\ &\times \exp \left(-\frac{L(m_1 \Gamma_1 + m_3 \Gamma_3)}{2E} \right) \left(1 - 2 \sin^2 \frac{\Delta m_{31}^2 L}{4E} \right) \\ &+ 2s_{12}^2 c_{13}^2 s_{13}^2 \exp \left(-\frac{L(m_2 \Gamma_2 + m_3 \Gamma_3)}{2E} \right) \left(1 - 2 \sin^2 \frac{\Delta m_{32}^2 L}{4E} \right) \end{aligned} \quad (5)$$

where $c_{ij}^n = \cos^n \theta_{ij}$ and $s_{ij}^n = \sin^n \theta_{ij}$.

After deriving our probability functions, we determined the total number of antineutrino events in each case. The JUNO experiment expects to detect over 100,000 electron antineutrino events over the span of 5–10 years (An et al. 2016), and we sought to model this. Electron antineutrinos are detected via inverse β -decay: $\bar{\nu}_e + p \rightarrow e^+ + n$. In the JUNO detector, the neutrino energy is determined using the measurement of the positron energy. The outgoing neutrons are also detected; the coincident detection of a positron and neutron allows JUNO to distinguish electron antineutrino events from background events (An et al. 2016).

The total number of antineutrino events is given by the product of P_{ee} , the neutrino cross section, and the neutrino flux. We obtained the cross section from Strumia & Vissani (2003). The neutrino flux, in arbitrary units, depends on the isotopes which produce the neutrinos. We determined the flux corresponding to each isotope using the methods outlined in Mueller et al. (2011), and we assumed JUNO's isotope ratios, given by An et al. (2016). We normalized our data sample to 100,000 events, which represents 5 years of JUNO data.

3. Results and Discussion

We first let the three neutrino mass eigenstates, $|\nu_1\rangle$, $|\nu_2\rangle$, and $|\nu_3\rangle$, decay individually, and then we let multiple states decay simultaneously. As shown in Figure 1, $|\nu_3\rangle$ decay suppresses the small oscillations, $|\nu_2\rangle$ decay suppresses the long oscillations, and $|\nu_1\rangle$ decay reduces the overall number of neutrino events. In the hybrid cases, we saw various decay effects, from which it can be predicted which neutrinos decayed.

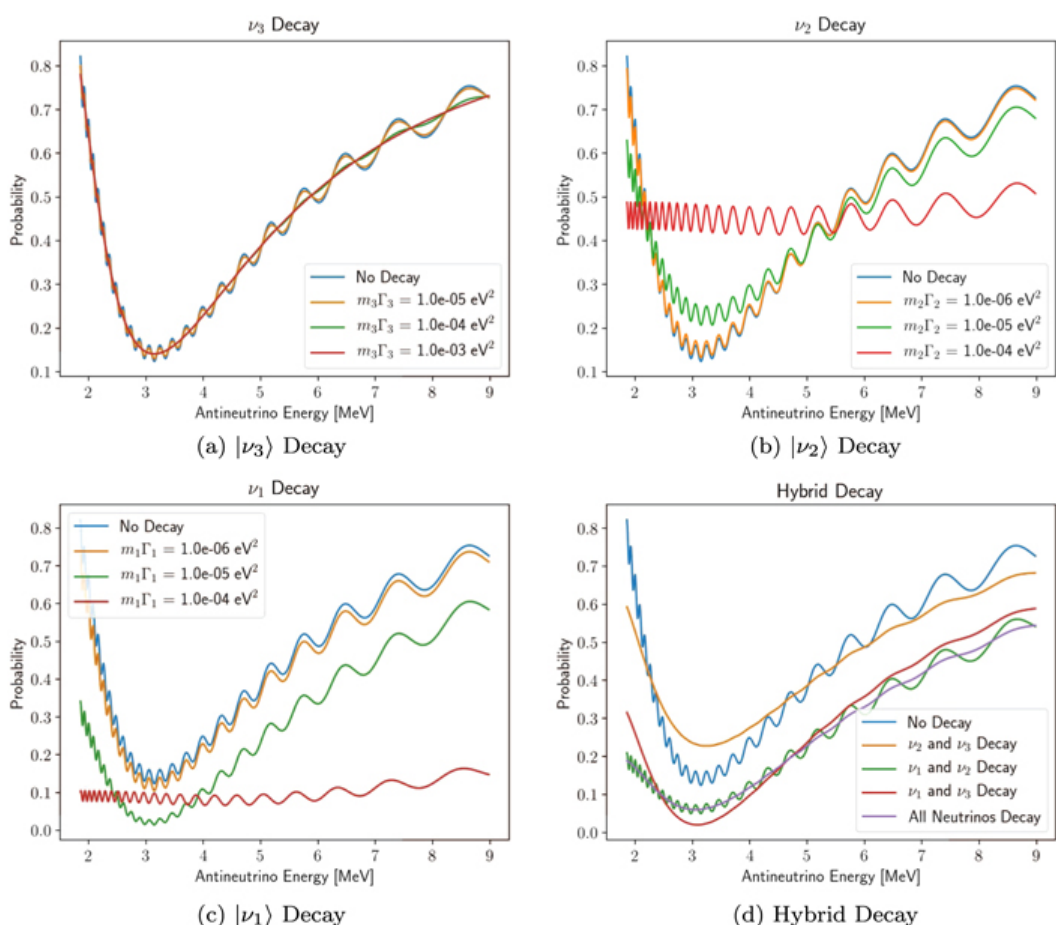


Figure 1. Effects of Neutrino Decay on Flavor Oscillations.

After determining the effect of neutrino decay on the shape of the oscillations, we compared our uncertainties in our oscillation parameters with JUNO's. We determined that our uncertainty is slightly better than JUNO's predictions (An et al. 2016), which we expect, as we did not account for background noise or the effects of JUNO's energy resolution in our simulations.³ We then used chi-square tests to set bounds on our decay factors. Using the 2σ statistic, we set our upper bounds as $7.39 \times 10^{-8} \text{ eV}^2$, $2.50 \times 10^{-7} \text{ eV}^2$, $6.52 \times 10^{-6} \text{ eV}^2$ for $m_1\Gamma_1$, $m_2\Gamma_2$, and $m_3\Gamma_3$, respectively. These results are obtained assuming the relevant oscillation parameters are known with infinite accuracy.

Once we cemented reasonable bounds on our decay factors, we looked for correlations between the decay factors and the other parameters using two-dimensional chi-square tests. We found the solar mixing angle (θ_{12}) has the strongest correlation with $m_1\Gamma_1$ and $m_2\Gamma_2$, and θ_{13} was correlated with $m_3\Gamma_3$. However, we did not pursue the second correlation, as there are strong constraints on θ_{13} from existing experiments (see An et al. 2017). Instead, we marginalized over $\sin^2 \theta_{12}$ in reduced chi-square tests, which enabled us to refine our decay factor estimates. Using the 2σ statistic, our improved upper bound estimates are $1.20 \times 10^{-7} \text{ eV}^2$, $4.45 \times 10^{-7} \text{ eV}^2$, $6.67 \times 10^{-6} \text{ eV}^2$, for $m_1\Gamma_1$, $m_2\Gamma_2$, and $m_3\Gamma_3$, respectively.

4. Conclusions

We first concluded that $|\nu_3\rangle$ decay suppresses the small neutrino oscillations, $|\nu_2\rangle$ decay suppresses the long oscillations, and $|\nu_1\rangle$ decay decreases the number of neutrino events. We then determined reasonable upper bounds for $m_1\Gamma_1$, $m_2\Gamma_2$, and $m_3\Gamma_3$. Currently, solar neutrino data constrains the invisible decays of ν_1 and ν_2 very strongly ($m\Gamma < 10^{-12} \text{ eV}^2$) (Berryman et al. 2015). The strongest constraint on the invisible decay of ν_3 comes from atmospheric neutrinos: $m_3\Gamma_3 < 3.3 \times 10^{-6} \text{ eV}^2$ at the two sigma level (Gonzalez-Garcia & Maltoni 2008). Our estimates indicate that JUNO can compete with the current upper bound for $m_3\Gamma_3$. While the solar experiments use only neutrinos, JUNO will observe only antineutrinos. Hence, by comparing the bounds on the neutrino and antineutrino lifetimes we can test the CPT-theorem (which says particles and antiparticles must have exactly the same lifetime). Similarly, the atmospheric neutrino result assumes the CPT-theorem since the data includes both neutrinos and antineutrinos, so the JUNO data are qualitatively different. Our results agree with those published in Abrahão et al. (2015), where a similar exercise was carried out. This indicates that our approximations are very reasonable.

This research was sponsored by NSF Grant 1757792.

Footnotes

³ This effect is partially captured in our choice to bin the data and make the bin widths similar to the detector's energy resolution.